2012

Simultaneous Heat and Mass Transfer in a Wetted Heat Exchanger, Part I: Experiments

Feini Zhang
fzhang8@illinois.edu

Jessica Bock

Anthony M. Jacobi

Hailing Wu

Simultaneous heat and mass transfer in a wetted heat exchanger, part I: experiments

Feini ZHANG [1]*, Jessica BOCK [1], Anthony M. JACOBI [1], Hailing WU [2]

[1] University of Illinois at Urbana Champaign, Department of Mechanical Science and Engineering, Urbana, Illinois, United States of America
Contact Information (fzhang8@illinois.edu)

[2] United Technologies Research Center
East Hartford, Connecticut, United States of America
Contact Information (WuHL@utrc.utc.com)

*Corresponding Author

ABSTRACT

Using an induced open-loop wind tunnel and a full cone water spray nozzle, the performance of a brazed aluminum heat exchanger with louvered fins is studied experimentally for wet conditions. The total capacity, pressure drop and water drainage behavior under various water usage rates and air face velocities are explored and compared to dry-condition data. The impact on spray orientation is also studied. The results are presented as plots of performance against water usage rate or water spray rate per unit heat transfer area. Fouling on the fin surface was observed in the experiment, and fouling distribution characteristics are discussed in this paper.

The experimental data are used to validate the model presented in "Simultaneous heat and mass transfer in a wetted heat exchanger, part II: modeling"

1. INTRODUCTION

Air-cooled heat exchangers are used in power plants and air conditioning and refrigeration systems. However, air-cooled systems show significant degradation in performance when the ambient temperature is high. This degradation is manifested as a decrease in COP (coefficient of performance) for air-conditioning and refrigeration systems, or as a decrease in thermal efficiency or generating capacity for a power plant. The performance of these air-cooled systems would be improved, if the air-side temperature could be lowered. One method to achieve that goal is to use evaporative cooling.

Hosoz and Kilicarslan (2004) found a system with a direct water-air hybrid cooled evaporative condenser (bare-tube heat exchanger) could give up to a 15.2% higher COP than that obtained with an air-cooled condenser. Other researchers have conducted experiments on residential air conditioners with an indirect evaporative cooled condenser using media pads (Goswami *et al.*, 1993) (Hajidavalloo, 2007). They saw significantly less electricity consumption compared to basic systems at high ambient temperature. An assessment of the cost and performance of spray nozzle pre-cooled, Munters media pre-cooled, spray nozzle and Munters media hybrid cooled and direct deluge cooled condensers for an air-cooled geothermal power plant in Nevada was conducted by Kutscher and Costenaro (2002). All four methods raised the summer output by at least 36%, but deluge cooling was found to be superior to the other three approaches. However, scaling and corrosion on the heat exchanger fins present a significant technical hurdle for deluge cooling. Qureshi and Zubair (2005) coupled their fouling growth model with an evaporative cooling model and predicted 50% and 70% decreases in effectiveness due to fouling for evaporative coolers and condensers, respectively.

Bare-tube heat exchangers dominate in the application of water/air evaporative cooling condensers when a direct spray is used, to try to avoid fouling and corrosion issues (Hosoz and Kilicarslan, 2004) (Kutscher and Costenaro, 2002). These issues would be alleviated if pure water is supplied. Recent developments of membrane distillation technology enables pure water production at a total operating cost of 0.56 $/m^3 utilizing low grade thermal energy (Curcio and Drioli, 2005). This makes compact heat exchangers with deluge cooling more promising choices to consider. To date, no investigations have been reported in the open literature on the performance of water/air hybrid cooling on compact heat exchangers.

Overspray is another issue that should be considered, since water carryover may create operational problems and certainly results in a waste of process water (Kutscher and Costenaro, 2002). Adding a water collection and recirculating system could increase the cost and space required. As a result, optimizing the water spray rate under various working conditions is needed.

In the experiments presented in this article, a lab-based hybrid-water/air evaporatively cooled compact heat exchanger system (Figure 1) was developed to optimize system operation with minimal water consumption. An atomizer was used as the air-side water distributer. A flat-tube, louver-finned heat exchanger was used in this experiment to investigate evaporative cooling process on the air-side surface. Evaporation rate, change of capacity and change of pressure drop were measured during the experiment. The data were used to validate the evaporative cooling model developed by Bock *et al*., 2012.

2. EXPERIMENTAL METHODS

2.1 Experimental Facility

The experiments were conducted in an open- circuit wind tunnel. Both dry and wet-surface cooling conditions were studied. A schematic diagram of the wind tunnel and refrigerant circulation circuit is shown in Figure 1. Ambient air entered through a flow straightener and contraction, passed a spray nozzle, went through the test heat exchanger, an axial blower, a flow nozzle, and then exited the tunnel. The cross-sectional dimensions of the wind tunnel were 305 mm × 203 mm. The face area of the test heat exchanger was 203 mm × 203 mm. A schematic diagram of the flat-tube, louver-fin heat exchanger is shown in Figure 2, with (a) close-up frontal view, and (b) cross-sectional view of louver fin. The detailed dimensions of the brazed exchangers used for this experiment are listed in Table 1. A two-dimensional contraction and diffuser with a contraction (diffusion) ratio of 1.5 were installed immediately upstream and downstream of the test heat exchanger. All the supply pipes, reservoirs, heat exchangers the wind tunnel walls (from the spray nozzle to the exit of the wind tunnel) were thermally insulated from the ambient. The wind tunnel was double insulated with two layers of 1.27 cm thick Buna-N/PVC foam. The tube-side circulation system was triple insulated with a total thickness of 1 cm Polyethylene Foam tape.

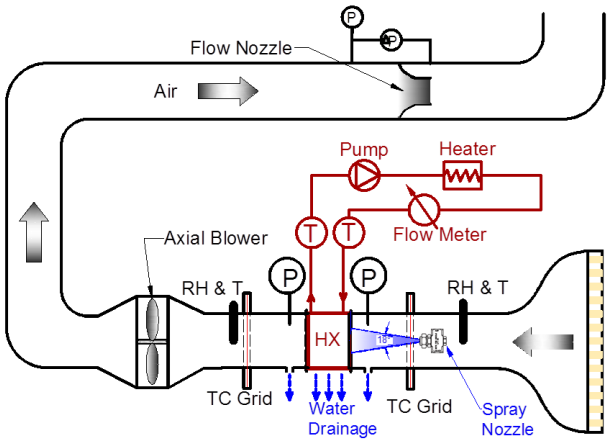

Figure 1: Wind tunnel schematic

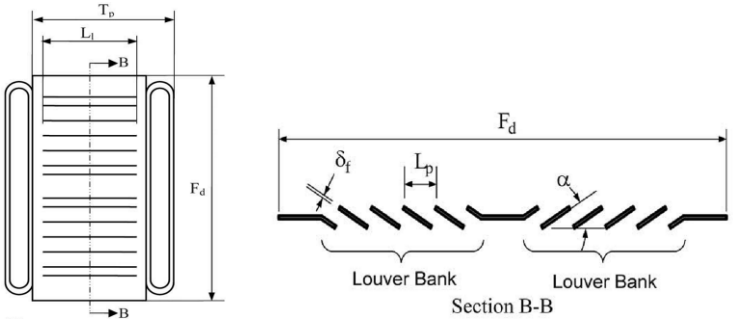

(a) (b)

Figure 2: Schematic diagram of a flat-tube, louver-fin heat exchanger:
(a) Tube-fin cross sectional view, (b) louver-fin cross sectional view (Park and Jacobi, 2009).

Table 1: Test heat exchanger geometry

L_p, louver spacing(mm)	2.21
L_l, louver length (mm)	6.67
θ, louver angle (deg)	30.6
F_p, fin spacing (mm)	2.125
F_d, fin depth (mm)	85.6
F_l, fin length (mm)	9.56
δ, fin thickness (mm)	0.33
T_p, tube spacing(mm)	11.88
Rows of tubes	19
T_h, tube height (mm)	1.65
T_d, tube depth (mm)	81
T_l, tube length (mm)	216
T_t, tube thickness	0.57

On the air side, an 18 degree full cone spray nozzle was located 28 cm upstream of the test heat exchanger at the center of the tunnel. The air temperature was measured using thermopile grids with T-type thermocouples, with 12 channels upstream and 29 channels downstream. Both temperature and relative humidity were recorded at the entrance and exit of the test section. Micro-manometers were used to measure air-side pressure drop through the heat exchanger. Downstream of the test section, an ASME standard long radius nozzle and differential pressure transducers were used to find air mass flow rate.

On the tube side, an ethylene glycol and water solution (56% vol. ethylene glycol) was used as heat transfer fluid. Both the inlet and outlet temperatures of the solution were measured using four thermocouples (two for out let and two for inlet). In the supply loop, a PID-controlled electric heater heated the liquid. In the return line, a Coriolis-effect mass flow meter was used to measure coolant mass flow rate.

The data acquisition system consisted of four NI 9213 modules for thermocouple input and one NI 9205 module for humidity sensor and pressure transducer input. These units were connected to a computer using a NI cDAQ-9178 USB chassis. Real-time process variables, namely thermocouple readings, and pressure and humidity sensor readings were displayed and arranged using a Labview program.

2.2 Test Procedure and Uncertainty Analysis

The tube-side inlet temperature was held at about 46°C using the PID-controlled electric heater, and the flow rate was maintained constant by the variable speed gear pump. The air-side face velocity was controlled by the blower. The flow rate of the siphon-fed fogging nozzle was controlled by a pressure regulator. The spray was 18 degrees full

cone, according to the manufacturer. The water was supplied from graduated cylinders outside the wind tunnel and sprayed into the wind tunnel. Two different types of spray nozzles were used: *1/4XA 00 SR 250 A* for low-flow-rate conditions and *1/4XA 00 SR 400 A* for high-flow-rate conditions. The total volume of sprayed water was determined from the volume change in the graduated cylinders. The liquid water temperature in the cylinders was measured using 6 thermocouples submerged in the water at different levels, and the average was taken as the sprayed water inlet temperature.

Using the data acquisition system, samples were recorded every 5 seconds. If all real-time data were constant within the measurement uncertainty for 10 minutes, then steady-state conditions were considered to prevail. For each steady-state condition, data were recorded over an 8 minute period, in order to provide a large number of samples for averaging. The recorded data included tube-side inlet and outlet temperatures; air-side upstream temperature and humidity, downstream temperature, and flow nozzle pressure drop. At the same time, the water that did not evaporate and drained from the test section was collected and measured using a graduated cylinder. The volume change of water in the graduated cylinders supplying the spray nozzle was also recorded. During the course of the experiments, water supply pressure changed slightly with the supply water volume in the graduated cylinders, leading to a change in the spray mass flow rate; this effect was did not violate the criterion described above for determining steady-state conditions, and it was accounted for in the uncertainty analysis.

The experimental conditions are given in Table 2. For each air velocity, steady-state data for various spray water flow rates were recorded. Data for dry-surface conditions (0 g/s spray nozzle water mass flow rate) were always obtained before spraying water. Then the spray nozzle was turned on and the water mass flow rate was varied.

Table 2: Test conditions

Air face velocity [m/s]				**Spray nozzle water mass flow rate [g/m2s]**		
1.8		0	0.24	0.36	0.66	1.03
2.3	Horizontal spray	0	0.21	0.30	0.36	1.03
	10^o upward spray	0	0.21	0.36	0.66	1.03
3.2		0	0.21	0.36	0.66	1.06
Tube-side mass flow rate		0.1054 ± 0.0001 kg/s				
Air-side inlet temperature		23.5 ± 0.3 °C				
Tube side inlet temperature		46.4 ± 0.2 °C				

Among all the experimental results, 83% of the data had air-side and tube-side capacity deviation within 20%, and the maximum deviation is 27% at high water spray rate. The uncertainty of air-side heat transfer rate and tube-side heat transfer rate, δQ_{air} and δQ_{ts} respectively, obeyed Eq. (1) for all test conditions.

$$\frac{\delta Q_{ts}}{\delta Q_{air}} \le 0.1 \quad (1)$$

According to Park *et al.* (2010), for such conditions, it is more reasonable to use Q_{ts} than Q_{avg} as the total capacity.

The tube-side temperatures were measured using thermocouples fixed on the outer- surface of the aluminum supply and discharge tubes, using polyimide tape and Arctic Silver 5 to enhance conduction heat transfer. The tubes with thermocouples are insulated. Since the thermocouples did not have direct contact with the tube-side liquid, a bias error associated with heat transfer between the tube and the lab was incurred. The data were corrected for this bias error using the analysis described below.

The Reynolds number varied from 3500 to 4500, and the Gnielinski correlation for forced convection in turbulent pipe flow was used to obtain the heat transfer coefficient and hence thermal resistance between the tube-side fluid and the inner tube wall. The thermal resistance associated with conduction through the tube wall was calculated using the properties of aluminum alloy and the dimensions of the tube, and the thermal resistance associated with

conduction through the insulation on the outside of the tube was likewise calculated. Conservatively assuming the outside surface of the insulation to be at laboratory temperature:

$$Q = \frac{T_{fluid} - T_{measure}}{R_{tube} + R_{conv}} = \frac{T_{measure} - T_{ambient}}{R_{insulation}} \tag{2}$$

Bias error:

$$\Delta_{bias} = T_{measure} - T_{fluid} \tag{3}$$

The measured tube-side fluid temperature was corrected.

$$T_{corrected} = T_{measure} - \Delta_{bias} \tag{4}$$

This correction is simplified, in that it only accounts for radial heat transfer by convection and conduction, axial heat transfer is neglected, contact resistance is neglected, radiation is neglected, natural convection in the laboratory is neglected, and all temperatures are assumed uniform. In order to account for such simplifications in the uncertainty analysis, half of Δ_{bias} is conservatively included in the corrected measurement uncertainty $\Delta_{corrected}$.

$$\Delta_{corrected} = \sqrt{\Delta^2_{precition} + (\Delta_{bias} / 2)^2} \tag{5}$$

The uncertainties of measured parameters are given in Table 3.

Table 3: Summary of measurement uncertainty in dry/wet conditions

Parameters	**Uncertainty (average)**	
$T_{air,in}$	±0.10°C	
$T_{air,out}$	±0.42 °C	
$T_{tube,in}$	Precision	±0.08°C
	Bias	-0.14 °C
	corrected	±0.10 °C
$T_{tube,out}$	Precision	±0.11 °C
	Bias	-0.05 °C
	corrected	±0.12 °C
$RH_{air,in}$	±0.05	
Flow nozzle pressure drop	±16 Pa	
Core pressure drop	±5 Pa	
Coolant mass flow rate	±0.08 g/s	
water spray volume	±22 mL/s	
water drainage	±0.05% of reading	

3. RESULTS AND DISCUSSIONS

The experimental data for dry and wet tests have been used to validate the model developed by Bock *et al.* (2012)

3.1 Drainage Behavior

The drainage rate was recorded in the wet heat exchanger experiment as important information for water augmented cooling applications. Figure 3 (a) shows the heat capacity increases with the spray nozzle mass flow rate. However the curve fit indicates that the increasing rate tended to decrease as more water was sprayed, which indicates that spraying rate increases faster than water evaporation rate, leading to an increasing rate of drainage, as shown in Figure 4. This result suggests that at high water spray rates, drainage collection and recirculation system should be used.

Figure 3(b) indicates that water drainage rate was more affected by the water spray rate than by the air velocity. However, it was observed that the air-side face velocity did influence the location where the water was drained. At 1.8 m/s air-side face velocity, most of the water was drained in front of the heat exchanger; while at 3.2 m/s, most of the water was drained at the back of the heat exchanger. Water was drained at a similar rate both at the front and back of the heat exchanger, at 2.3 m/s air-side face velocity.

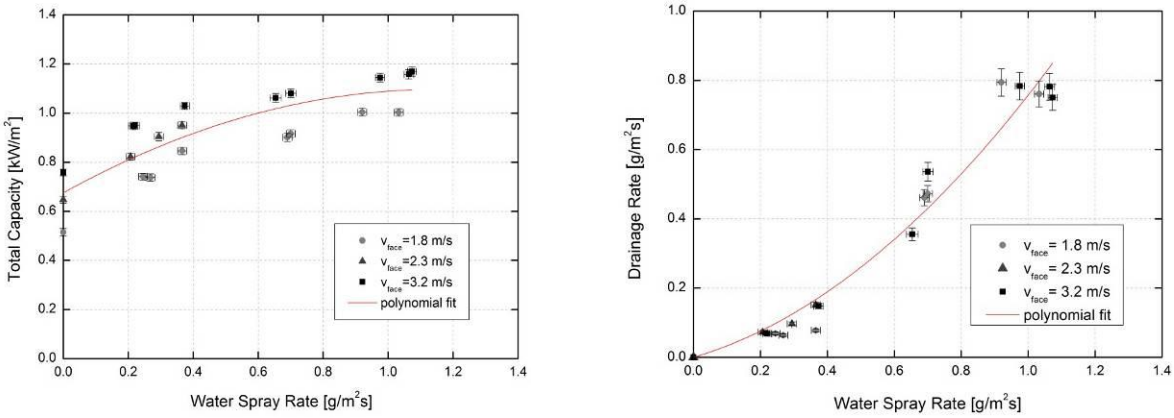

(a) **(b)**

Figure 3: Experimental data for 1.8 m/s, 2.3 m/s and 3.2 m/s heat exchanger air-side face velocity at various water spray rates. Water spray rate is defined as spray nozzle water mass flow rate. The second order polynomial curve fits are for all the data.

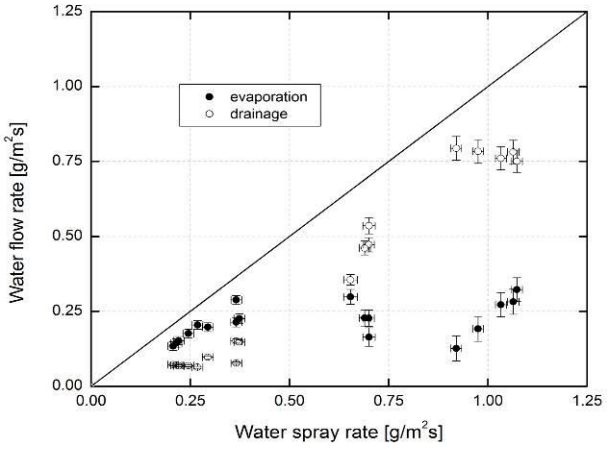

Figure 4: Comparison among water flow rates: total water spray rate, evaporation rate and drainage rate for all test conditions. The 45o line is water flow rate versus water flow rate itself.

3.2 Influence of Spray Orientation

At 2.3 m/s face velocity, both a horizontal spray and a spray directed 10 degrees up from horizontal were tested at various water spray rates. Comparison between the horizontally orientated spray nozzle and with 10 degrees angle upward is presented in Figure 5. The solid points and open circles are experimental data with horizontal nozzle orientation and corresponding model predictions with uniform water distribution at the heat exchanger front surface. The triangles are experimental data for 10 degree upward orientated nozzle conditions. The points at mw=0 g/(m^2-s) are dry condition data. As shown in Figure 5, the 10 degrees upward condition shows 4% to 12 % larger heat capacity than the horizontal oriented spray. This result is expected, because when water is directed at the upper part of the heat exchanger it drains toward the bottom of the heat exchanger due to gravity and hence likely wets more surface area with an increase in residence time. This enhances the latent heat transfer. In the horizontal case, roughly 40% of the heat exchanger face area was wet, while in the upward spray case more than 50% was wet. This result confirms that, the upward orientation is more effective and is preferred for practical water augmentation application.

Pressure drop under dry and wet conditions was measured in the experiment. As indicated in Figure 6, the heat exchanger air-side pressure drop gets larger as the Reynolds number increases. In the figure, the pressure drop under wet conditions is consistently higher than under dry conditions; however this difference is insignificant. Figure 7 shows that the pressure drop cross the test heat exchanger is mainly dependent on the air face velocity, and is barely affected by the total water usage rates.

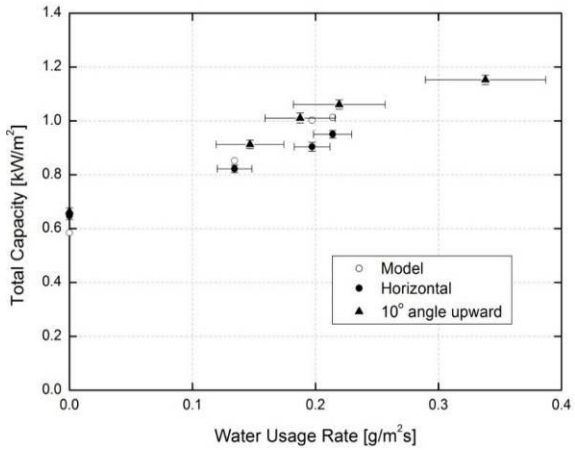

Figure 5: Comparison of total capacity between the horizontally orientated spray nozzle and 10 degrees angle upward spray conditions.

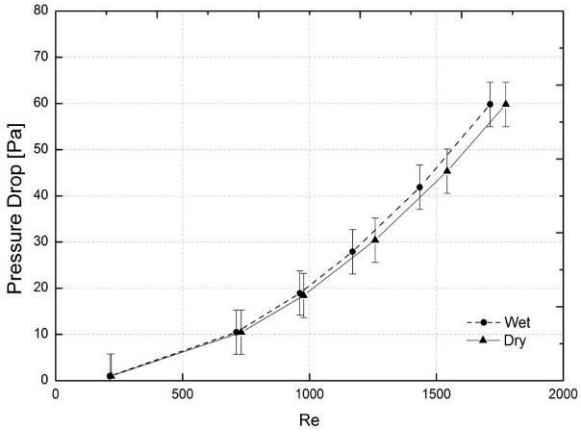

Figure 6: Comparison between wet test (with water spray rate about 0.12 g/m2s) and dry test pressure drop for varies Reynolds number.

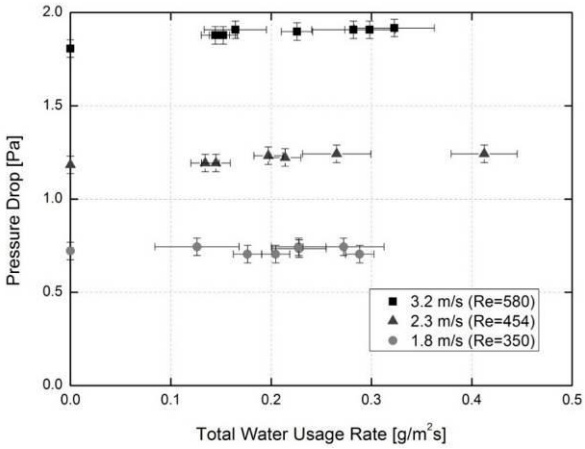

Figure 7: The test heat exchanger pressure drop at varies total water usage rates

3.3 Observation of Fouling

Pictures of the front and back view of the heat exchanger were taken before and after the test. Comparing to the image before test, as shown in Figure 8, it is found at the end of the experiment that, fouling exists at the front surface of the test heat exchanger where the fins were wet. However the center region, where is always directly wetted by the cone of the spray (full cone), has much less fouling than the wet region arround. The fouling region is shown in Figure 8(b). At the back of the test heat exchanger, more fouling occurs at the bottom, as shown in Figure 8(d). This fouling pattern is expected since the water slowly drained downward by gravity. More water stayed on the fins at the lower part of the heat exchanger, leading to more severe fouling. Figure 8 (b) and (d) were taken after about 2 months on-and-off spray testing (with spray time of less than 100 hours). It should be noted that tapwater was used for spray, which was high in chlorine and iron.

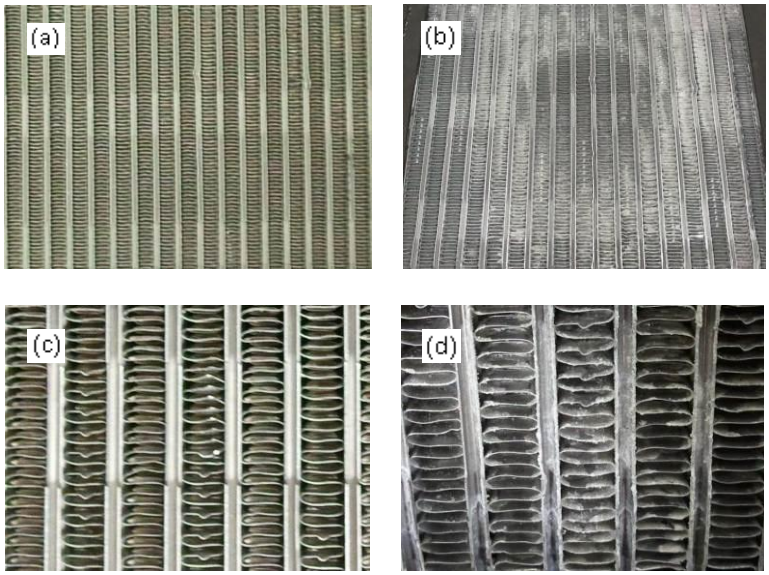

Figure 8: The heat exchanger surface:
(a) front surface before the wet condition experiment, (b) front surface after the wet experiment;
(c) back surface before the wet condition experiment, (d) back surface after the wet experiment.

4. CONCLUSIONS

Using an induced open-loop wind tunnel and a full cone water spray nuzzle, the performance of a brazed aluminum heat exchanger with louvered fins was studied experimentally for spray deluge cooling. The total capacity, pressure drop and water drainage behavior under various water usage rates and air face velocities were explored and compared to dry-surface data.

- It was found that both heat capacity and the mass flow rate of water drainage increased as more water was sprayed. At high water spray rates, a drainage collection and recirculation system should be used.
- Pressure drop under wet conditions was consistently but insignificantly higher than under dry conditions, and the pressure drop was independent of water usage rate in the range of the test conditions.
- It was found that the percentage of drained water was more affected by the water spray rate than by the air velocity. However, water tended to drain downstream at higher air velocity in the range of the test conditions.
- The impact of spray orientation was also studied. The upward orientation was more effective and is preferred for practical water augmentation application.

Fouling on the fin surface was observed in the experiment where the fins were wet. The center region of the front surface, where the heat exchanger was always directly wetted by the cone of the spray (full cone), had much less fouling than the wet region around it. At the back of the test heat exchanger, more fouling occured at the bottom.

NOMENCLATURE

C	Specific heat	(J/kg-k)	**Subscripts**	
F	Fin	(mm)	a	air
L	Louver	(mm)	conv	convection heat transfer
m	Mass flow rate	(kg/s)	d	Depth
P	Pressure	(Pa)	da	dry air
Q	The heat flux of tube-side fluid to the ambient	(J/m^2)	face	Heat exchanger face
			fluid	heat exchanger tube-side fluid
R	Thermal resistance	(kg-K/J)	h	Height
T	Temperature; tube	(K)	l	Length
TC	Thermocouple		p	Pitch
V	Velocity	(m/s)	r	Refrigerant
			t	Thickness
Greek Symbols			ts	Tube side
α	Enthalpy	(J/kg)	tube	Heat exchanger tube
Δ	Uncertainty or difference		w	Water
δ	Thickness; differential		wb	Wet bulb
θ	Louver angle	(degree)		

REFERENCES

Hosoz, M., Kilicarslan, A., 2004, Performance evaluations of refrigeration systems with air-cooled, water-cooled and evaporative condensers, *Int. Energ. Res.*, vol. 28, no. 8 : p. 683-696

Goswami, D.Y., Mathur, G. D., Kulkarni, S. M., 1993, Experimental investigation of Performance of a Residential Air Conditioning System with an Evaporatiyely Cooled Condenser, *ASME Transcation*, vol. 115 : p. 206-211.

Hajidavalloo, E., 2007, Application of evaporative cooling on the condenser of window-air-conditioner, *Appl. Therm. Eng.*, vol. 27, no. 11-12: p. 1937–1943.

Kutscher, C., Costenaro, D., 2002, Assessment of Evaporative Cooling Enhancement Methods for Air-Cooled Geothermal Power Plants,*GRC*.

Bock J., Zhang F., Jacobi A. M., Wu H., 2012, Simultaneous heat and mass transfer in a wetted heat exchanger, Part II: Modeling, *Purdue Conference*.

Qureshi, B. A., Zubair, S. M., 2005, The impact of fouling on performance evaluation of evaporative coolers and condensers, *Int. Energ. Res.*, vol. 29, no. 14: p. 1313-1330.

Curcio E., Drioli E., 2005, Membrane Distillation and Related Operations—A Review, *Sep. Purif. Rev.*, vol. 34, no. 1: p. 35–86.

Park Y. G., Jacobi A. M., 2009, The Air-Side Thermal-Hydraulic Performance of Flat-Tube Heat Exchangers With Louvered, Wavy, and Plain Fins Under Dry and Wet Conditions, Journal of Heat Transfer, Vol. 131, no. 6: 061801.

Park Y. G. , Liu L., Jacobi A. M., 2010, Rational approaches for combining redundant independent measurements to minimize combined experimental uncertainty, *Exp. Therm. Fluid Sci.*, vol. 34, no.6: p. 720-724.

ACKNOWLEDGEMENT

This material is based upon work supported by the Department of Energy [Geothermal Technologies Program] under award DE-EE0002738 [Optimization of Hybrid-water/air-cooled Condenser in an Enhanced Turbine Geothermal ORC System] to the United Technologies Research Center (PI: Dr. Hailing Wu). This paper was prepared as an account of work sponsored by an agency of the United States Government. Neither the United States Government nor any agency thereof, nor any of their employees, makes any warranty, express or implied, or assumes any legal liability or responsibility for the accuracy, completeness, or usefulness of any information, apparatus, process, or process disclosed, or represents that its use would infringe privately owned rights. Reference

herein to any specific commercial product, process, or service by trade name, trademark, manufacturer, or otherwise does not necessarily constitute or imply its endorsement, recommendation, or favoring by the United States Government or any agency thereof. The views and opinions of authors expressed herein do not necessarily reflect those of the United States Government or any agencies thereof. The authors are grateful for the support of the Department of Energy (DOE).